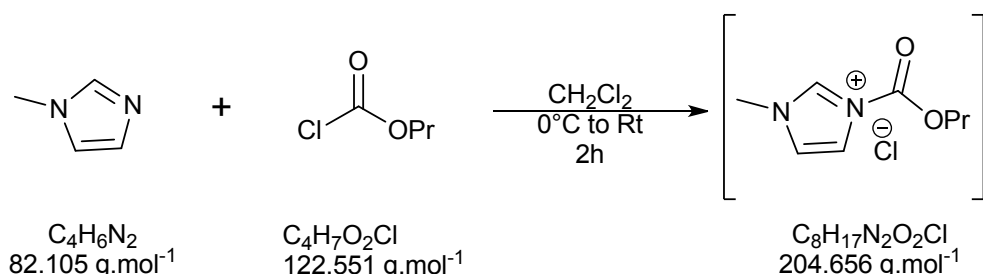


New route to carbonate-functionalized imidazolium and pyrrolidinium-based ionic liquids

Hassan Srour,^{a*} Walid Darwich,^a Felix Lindl,^a Pascale Husson,^c Helene Rouault,^b and Catherine Santini^a

Synthesis and characterizations

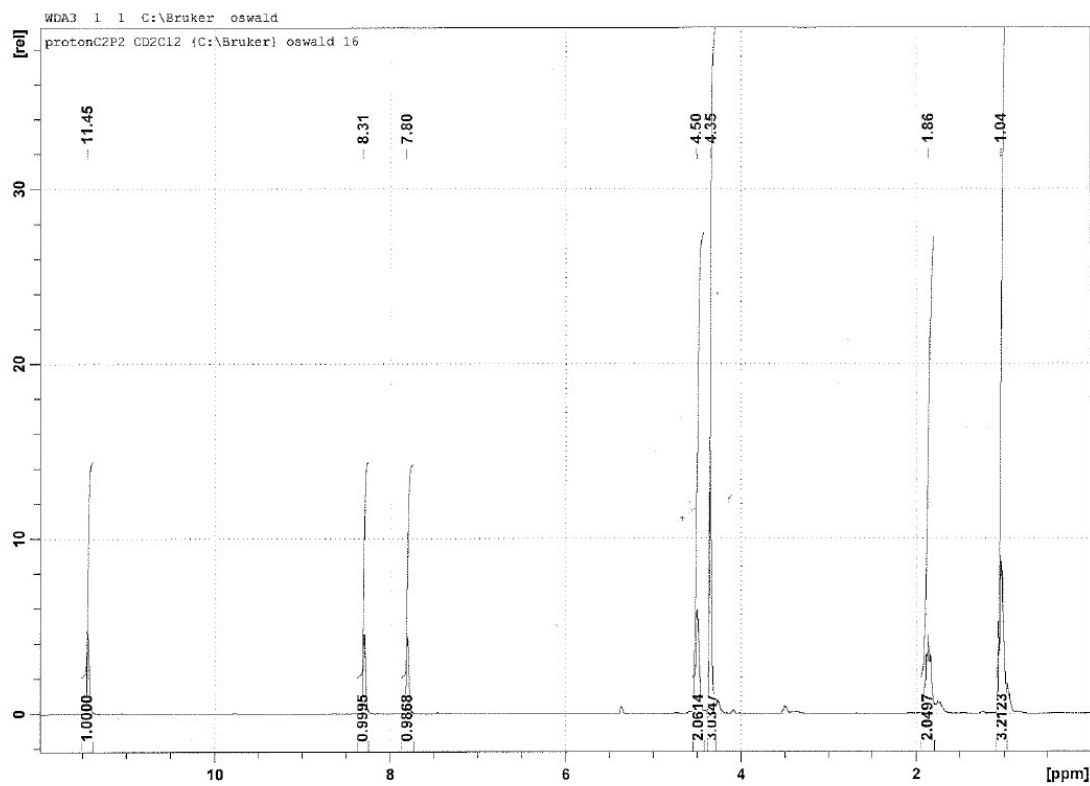
Formation of 3-methyl-1-(propyloxycarbonyl)imidazolium chloride intermediate (**1**)



The reaction was carried out under inert gas atmosphere. A solution of Propyl chloroformate (1.317 g, 1.208 mL, 10.749 mmol) in anhydrous CH₂Cl₂ (2 mL) was added drop wise at 0°C to a solution of 1-Methylimidazole (0.802 g, 0.779 mL, 9.772 mmol) in dried CH₂Cl₂ (2 mL). The mixture was warmed to room temperature and stirred for 2 h. Thereafter, the solvent was smoothly removed under vacuum. A colourless precipitate was performed (2.000 g, 9.772 mmol, 100%). The obtained solid was used for synthesis of **4** and **5** without further purification.



Scheme 1: The white precipitate of compound **1** intermediate.



Scheme 2: Proton NMR of the compound **1** intermediate.

CENTRE COMMUN DE SPECTROMETRIE DE MASSE

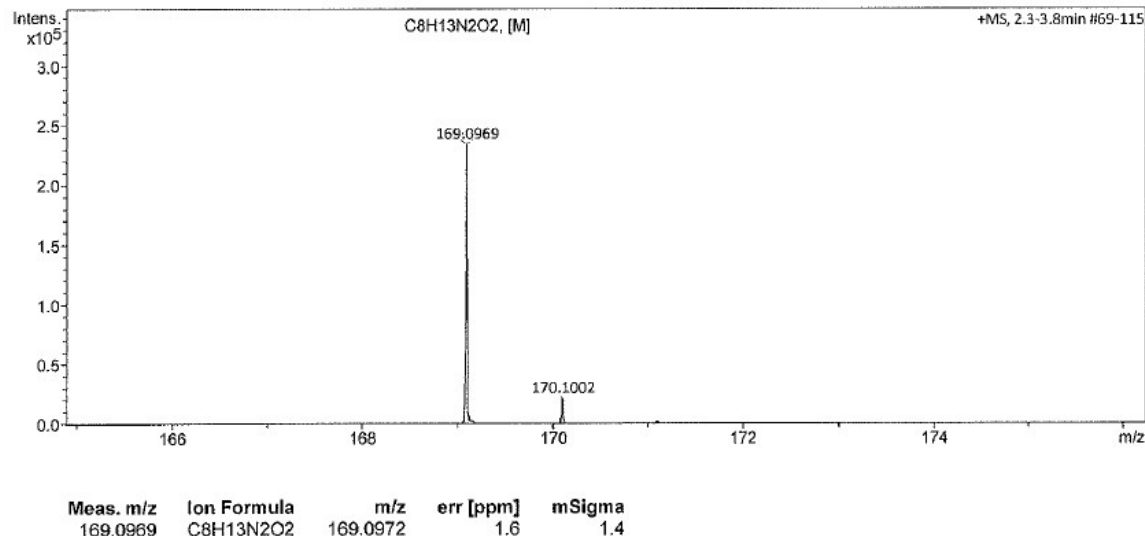
Analysis Info

Analysis Name QTOF170822_01_BM27.d
Method 2016_03_17_Infusion_50-1000_pos.m
Comment

Acquisition Date 8/22/2017 8:08:10 AM
Instrument / Ser# micrOTOF-Q 228888.10
231

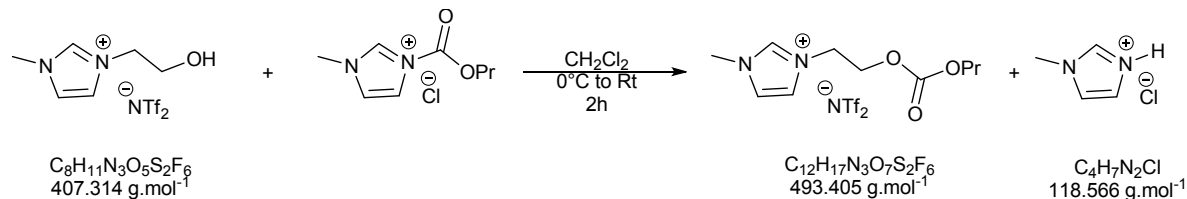
Acquisition Parameter

| | | | | | |
|-------------|----------|-----------------------|-----------|------------------|-----------|
| Source Type | ESI | Ion Polarity | Positive | Set Nebulizer | 0.4 Bar |
| Focus | Active | Set Capillary | 3500 V | Set Dry Heater | 200 °C |
| Scan Begin | 50 m/z | Set End Plate Offset | -500 V | Set Dry Gas | 4.0 l/min |
| Scan End | 1000 m/z | Set Collision Cell RF | 400.0 Vpp | Set Divert Valve | Waste |



Scheme 3: ESI⁺ of intermediate **1**, m/z=169 corresponding to the compound **1**.

Formation of 1-[2-(propyloxycarbonyloxy)ethyl]-3-methylimidazolium bis(trifluoromethane)sulfonimide (**4**) : $[C_1C_2O(CO)OPrIm][NTf_2]$



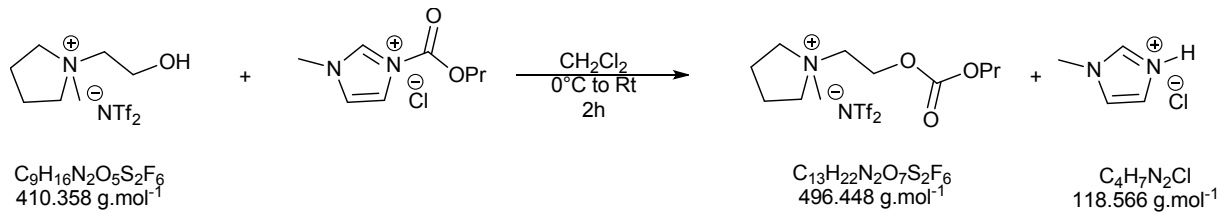
Via syringe 1-[2-(Hydroxy)ethyl]-3-methylimidazolium bis(trifluoromethane)sulfonimide (3.619 g, 8.885 mmol) was added drop wise to freshly generated precipitate **1** (2.000 g, 9.772 mmol) at 0 °C. The resulting clear solution was warmed to 50 °C and stirred overnight. After cooling to room temperature, CH_2Cl_2 (9 mL) was added. The organic phase was washed with deionised water until no chloride was detected in the aqueous phase (AgNO_3 standard test). Evaporation of CH_2Cl_2 yielded a colourless viscous fluid (3.534 g, 7.164 mmol, 81 %).

$^1\text{H-NMR}$ (CD_2Cl_2): δ (ppm): 8.76 (s, 1H, C2H); 7.33 (d, 2H, C4H, C5H); 4.48 (m, 4H, $\text{NCH}_2\text{CH}_2\text{O}$); 4.09 (t, 2H, $\text{OCH}_2\text{CH}_2\text{CH}_3$); 3.95 (s, 3H, NCH_3); 1.67 (st, 2H, $\text{OCH}_2\text{CH}_2\text{CH}_3$); 0.94 (t, 3H, $\text{OCH}_2\text{CH}_2\text{CH}_3$).

$^{13}\text{C}[^1\text{H}]$ -NMR (CD_2Cl_2): δ (ppm): 155.0 ($\text{O}(\text{CO})\text{O}$); 136.9 (C2H); 124.3 (C5H); 123.2 (C4H); 120.2 (CF₃); 70.4 ($\text{OCH}_2\text{CH}_2\text{CH}_3$); 65.6 ($\text{NCH}_2\text{CH}_2\text{O}$); 53.8 ($\text{NCH}_2\text{CH}_2\text{O}$); 36.2 (NCH_3); 21.9 ($\text{OCH}_2\text{CH}_2\text{CH}_3$); 9.6 ($\text{OCH}_2\text{CH}_2\text{CH}_3$).

Electrospray, MS (+ve): m/z 213 (100% - $[\text{C}_1\text{C}_2\text{O}(\text{CO})\text{OPrIm}]^+$), MS (-ve): m/z 280 (100% - $[\text{NTf}_2]^-$).

Formation of N-methyl-N-[2-(propyloxycarbonyl)ethyl]pyrrolidinium bis(trifluoromethane)sulfonimide (**5**) : $[C_1C_2O(CO)OPrPy][NTf_2]$



Via syringe N -Methyl-N-[2-(Hydroxy)ethyl]-pyrrolidinium bis(trifluoromethane)sulfonimide (3.620 g, 8.822 mmol) was added drop wise to freshly generated precipitate **1** (2.000 g, 9.772 mmol) at 0 °C. The resulting clear solution was warmed to 50 °C and stirred overnight. After cooling to room temperature, CH_2Cl_2 (9 mL) was added. The organic phase was washed with deionised water until no chloride was detected in the aqueous phase (AgNO_3 standard test). Evaporation of

CH_2Cl_2 yielded slightly yellowish oil (3.478 g, 7.006 mmol, 79 %).

^1H -NMR (CD_2Cl_2): δ (ppm): 4.55 (m, 2H, $\text{NCH}_2\text{CH}_2\text{O}$); 4.13 (t, 2H, $\text{OCH}_2\text{CH}_2\text{CH}_3$); 3.72 (t, 2H, $\text{NCH}_2\text{CH}_2\text{O}$); 3.59 (m, 4H, C_2H_2 , C_5H_2); 3.12 (s, 3H, NCH_3); 2.28 (m, 4H, C_3H_2 , C_4H_2); 1.69 (st, 2H, $\text{OCH}_2\text{CH}_2\text{CH}_3$); 0.95 (t, 3H, $\text{OCH}_2\text{CH}_2\text{CH}_3$).

$^{13}\text{C}\{{}^1\text{H}\}$ -NMR (CD_2Cl_2): δ (ppm): 154.7 ($\text{O}(\text{CO})\text{O}$); 120.3 (CF_3); 70.5 ($\text{OCH}_2\text{CH}_2\text{CH}_3$); 65.6 (C_2H_2 , C_5H_2); 62.7 ($\text{NCH}_2\text{CH}_2\text{O}$); 61.7 ($\text{NCH}_2\text{CH}_2\text{O}$); 48.6 (NCH_3); 21.9 (C_3H_2 , C_4H_2); 21.3 ($\text{OCH}_2\text{CH}_2\text{CH}_3$); 9.7 ($\text{OCH}_2\text{CH}_2\text{CH}_3$).

Electrospray, MS (+ve): m/z 216 (100% - $[\text{C}_1\text{C}_2\text{O}(\text{CO})\text{OPrPy}]^+$), MS (-ve): m/z 280 (100% - $[\text{NTf}_2]^-$).

Appendix A

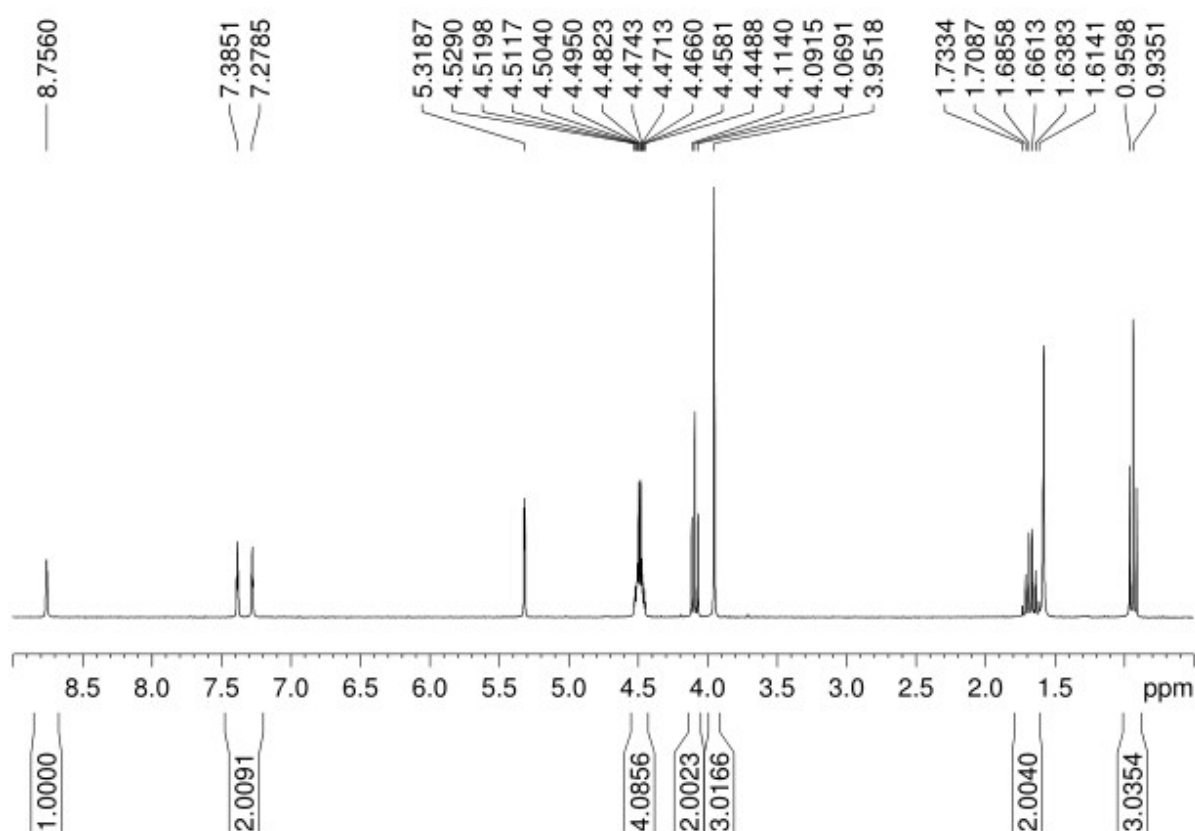


Fig A1 ¹H NMR spectra of ionic liquid **4**.

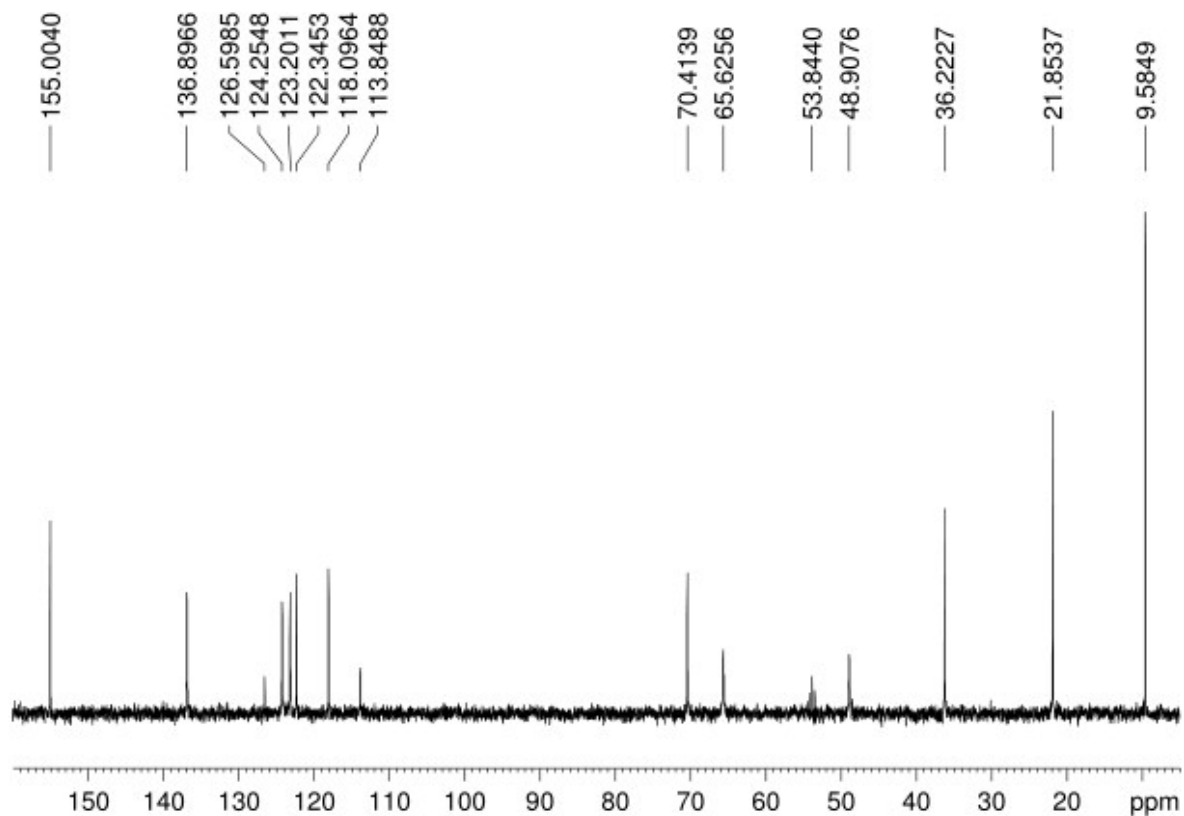


Fig A2 ¹³C NMR spectra of ionic liquid **4**.

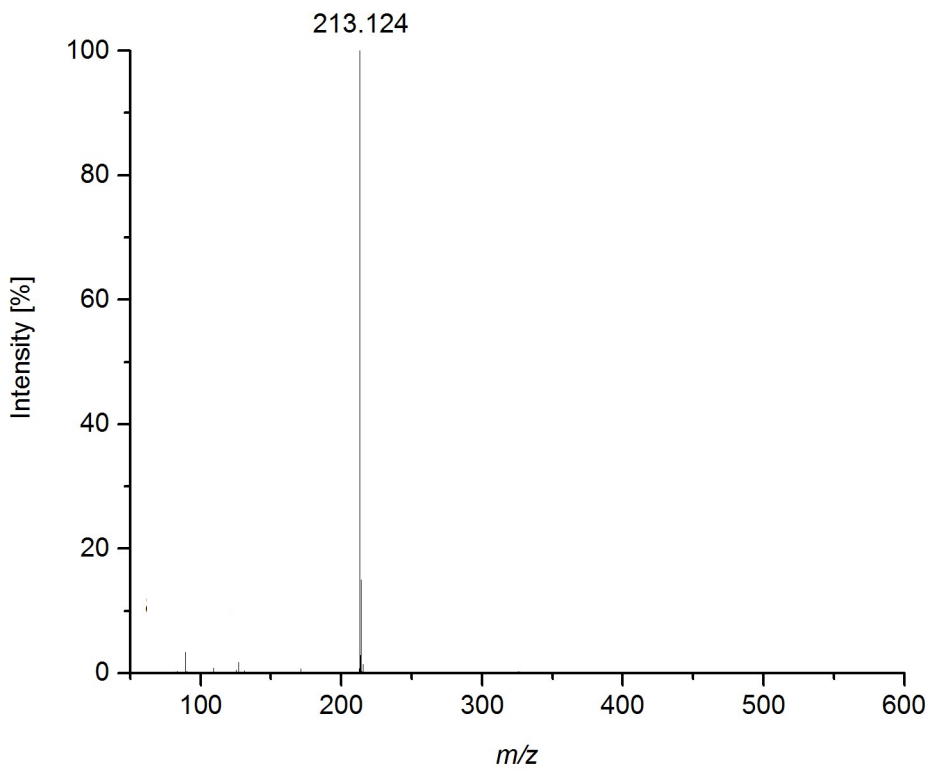


Fig A3 ESI⁺ spectra of ionic liquid **4**. Chloride cluster $[C_1(C_2O(CO)OC_3)Im]_2[Cl]$ peak at *m/z* = 461 is absent.

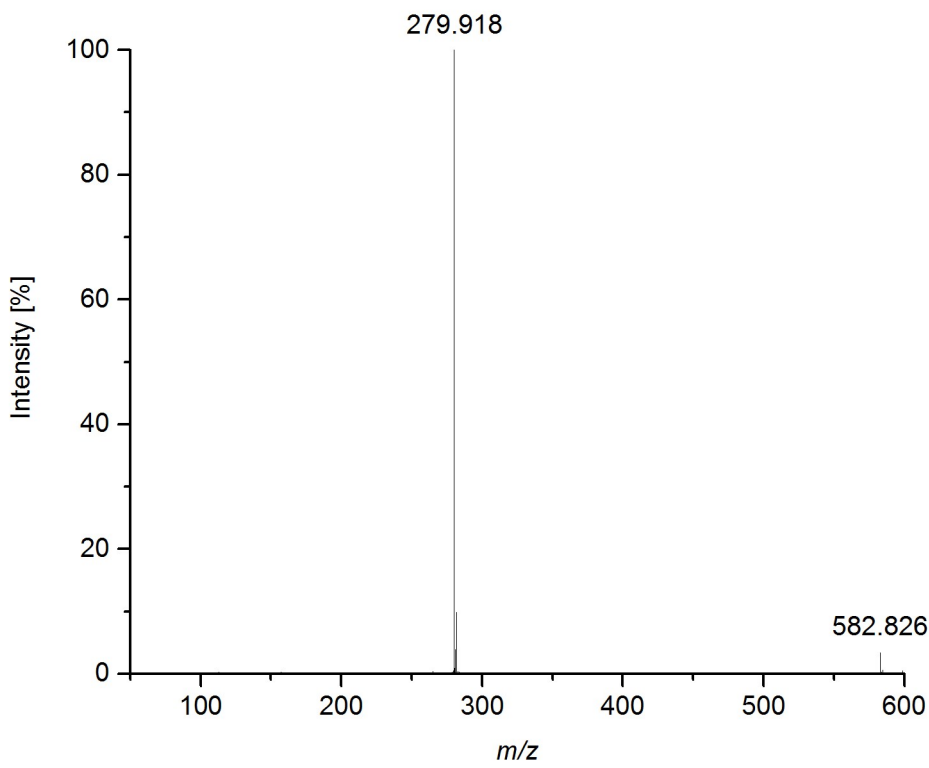


Fig A4 ESI⁻ spectra of ionic liquid **4**.

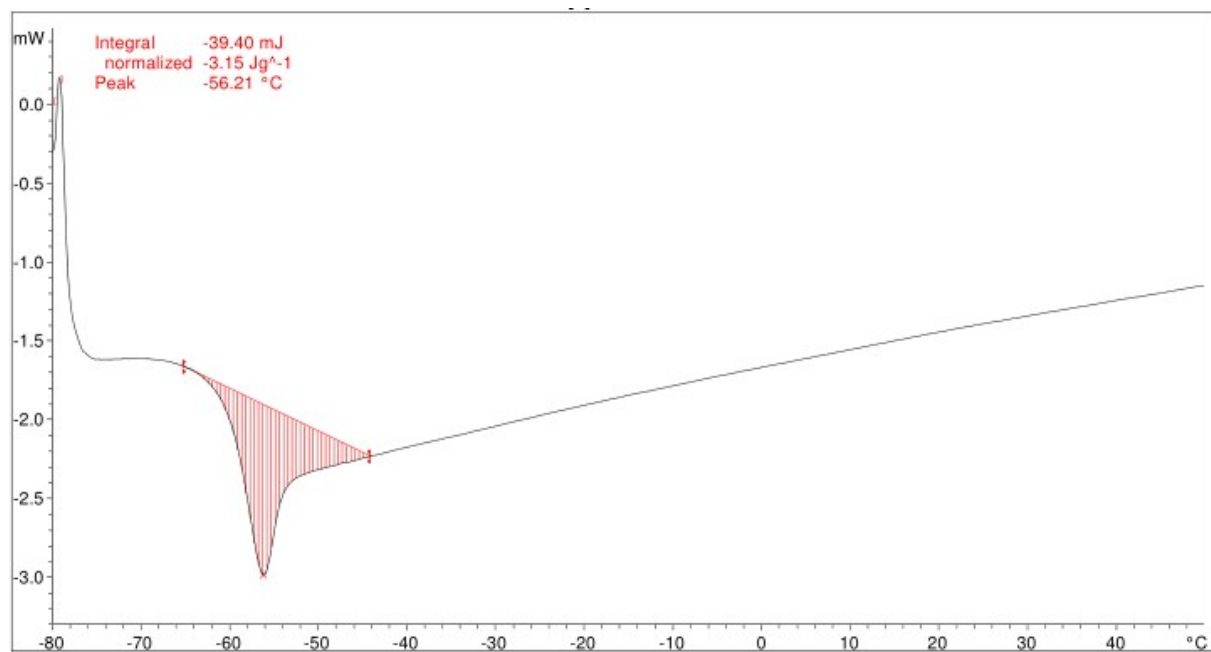


Fig A5 DSC spectra of ionic liquid **4**.

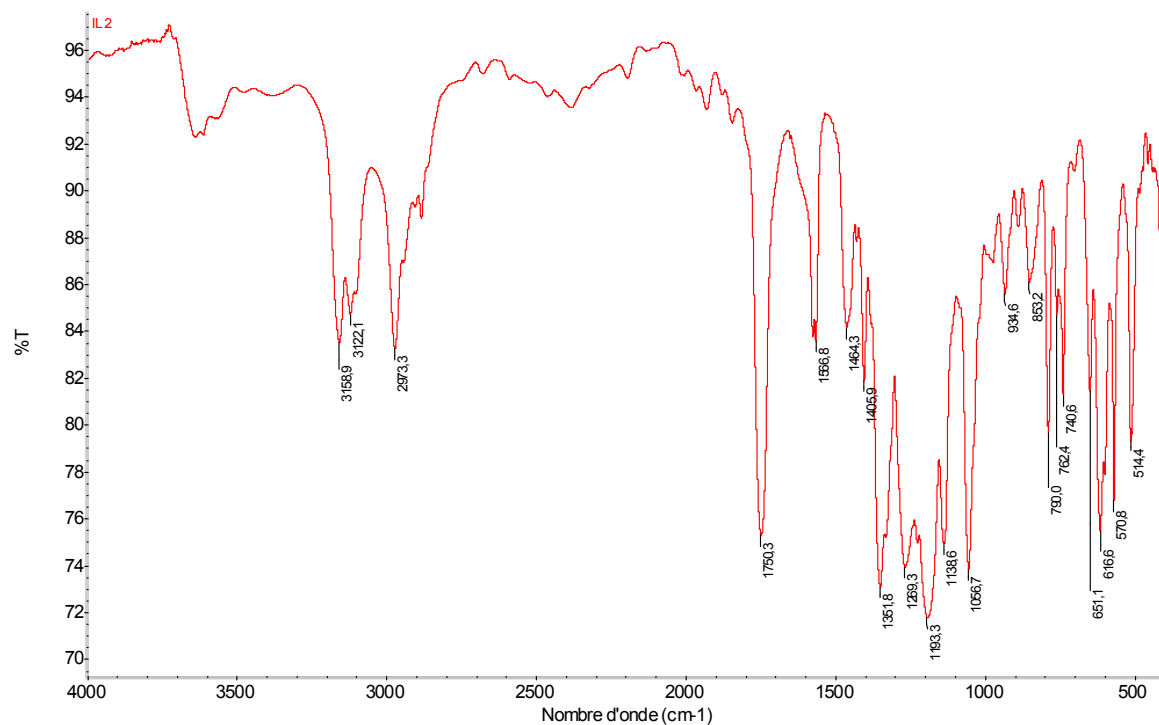
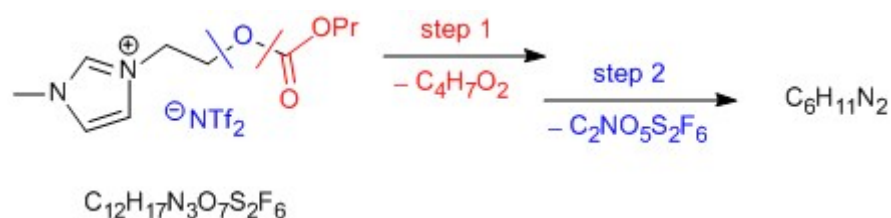
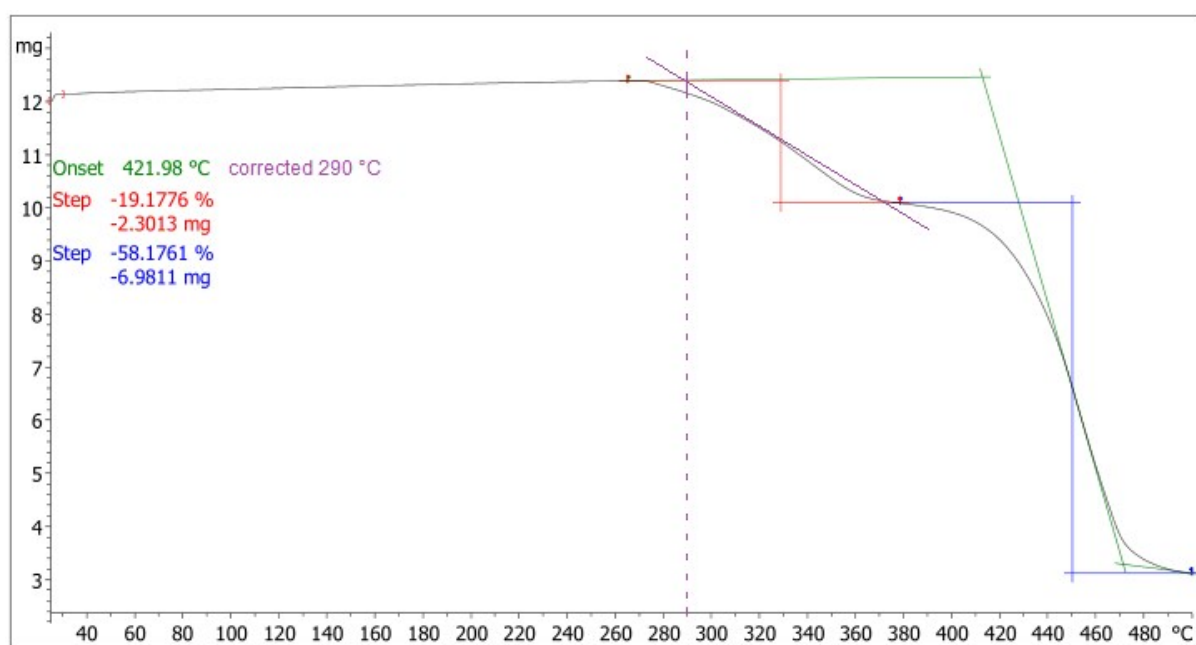


Fig A6 Infrared spectra of IL4.



| $\text{C}_{12}\text{H}_{17}\text{N}_3\text{O}_7\text{S}_2\text{F}_6$ (5) | m_{lost} theoret. | m_{lost} found |
|--|----------------------------|-------------------------|
| Step 1: $\text{C}_4\text{H}_7\text{O}_2$ | 17.6 % | 19.1 % |
| Step 2: $\text{C}_2\text{NO}_5\text{S}_2\text{F}_6$ | 60.0 % | 58.1 % |
| $\sum m_{\text{lost}}$ | 77.6 % | 77.2 % |

Fig A7 Thermogram of **IL4** demonstrates onset point, corrected onset point and two steps of decomposition.

Appendix B

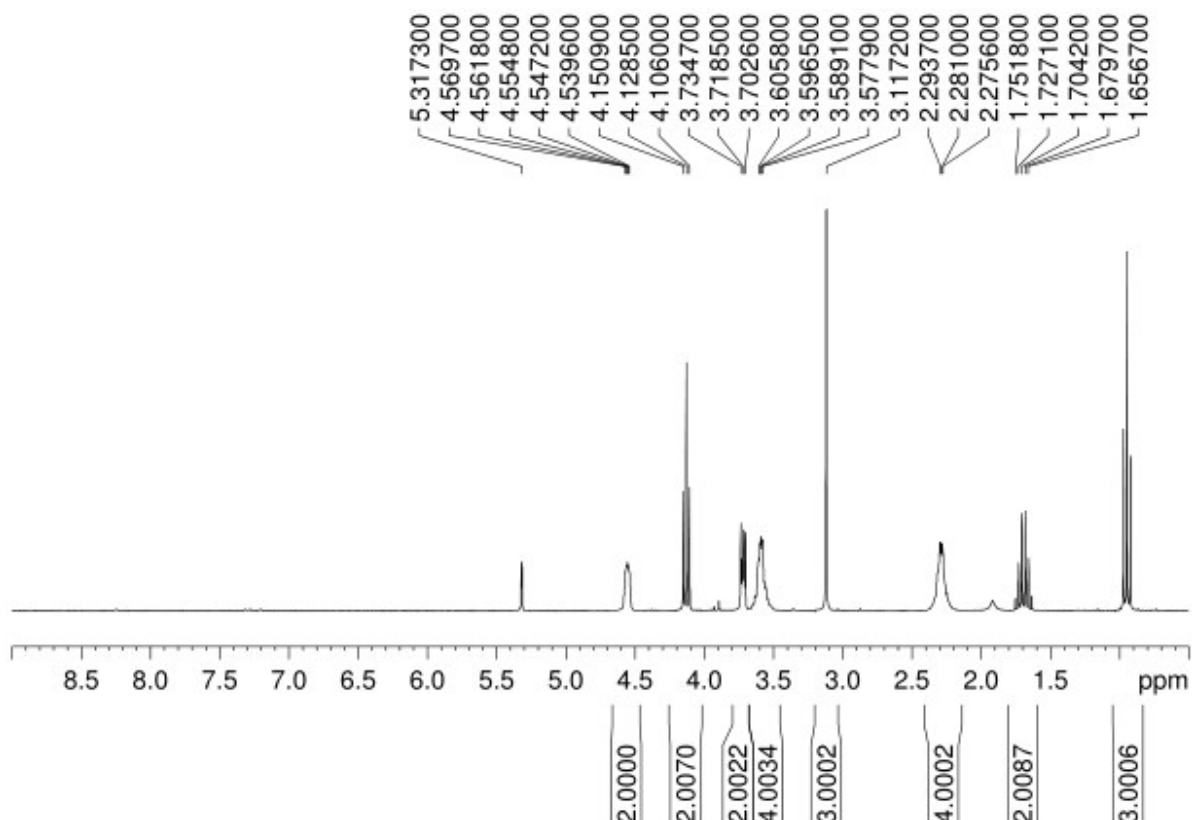


Fig B1. ¹H NMR spectra of IL5.

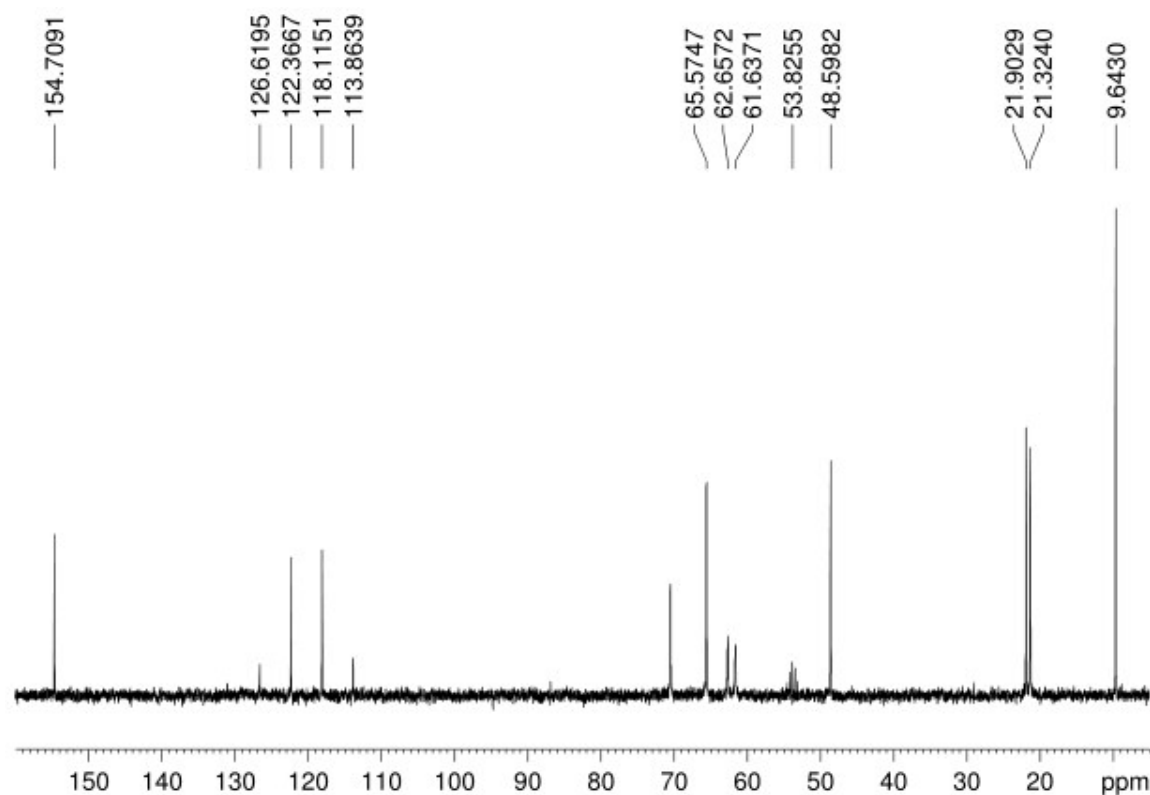


Fig B2. ^{13}C NMR spectra of **IL5**.

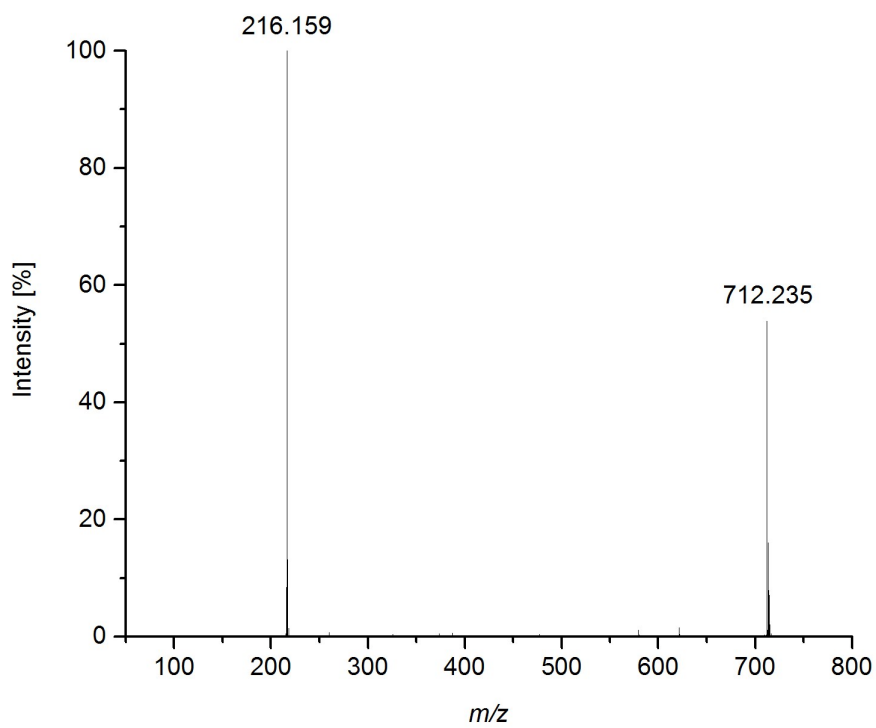


Fig B3. ESI $^+$ spectra of **IL5**. Chloride cluster $[\text{C}_1(\text{C}_2\text{O}(\text{CO})\text{OC}_3)\text{Py}]_2[\text{Cl}]$ peak at $m/z = 467$ is absent.

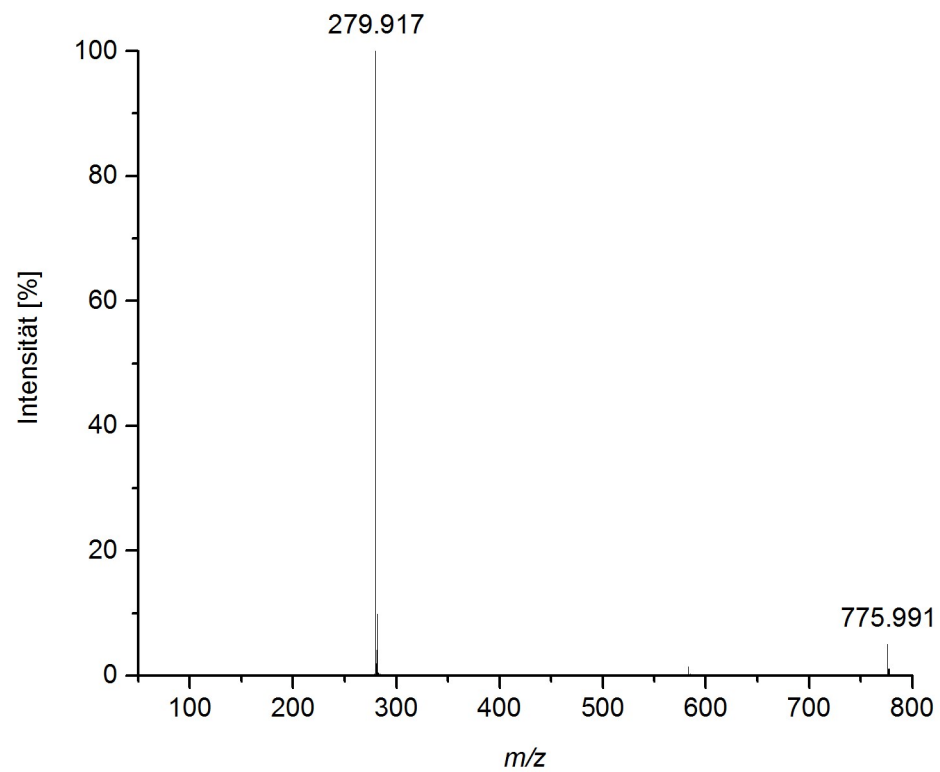


Fig B4 ESI⁻ spectra of **IL5**.

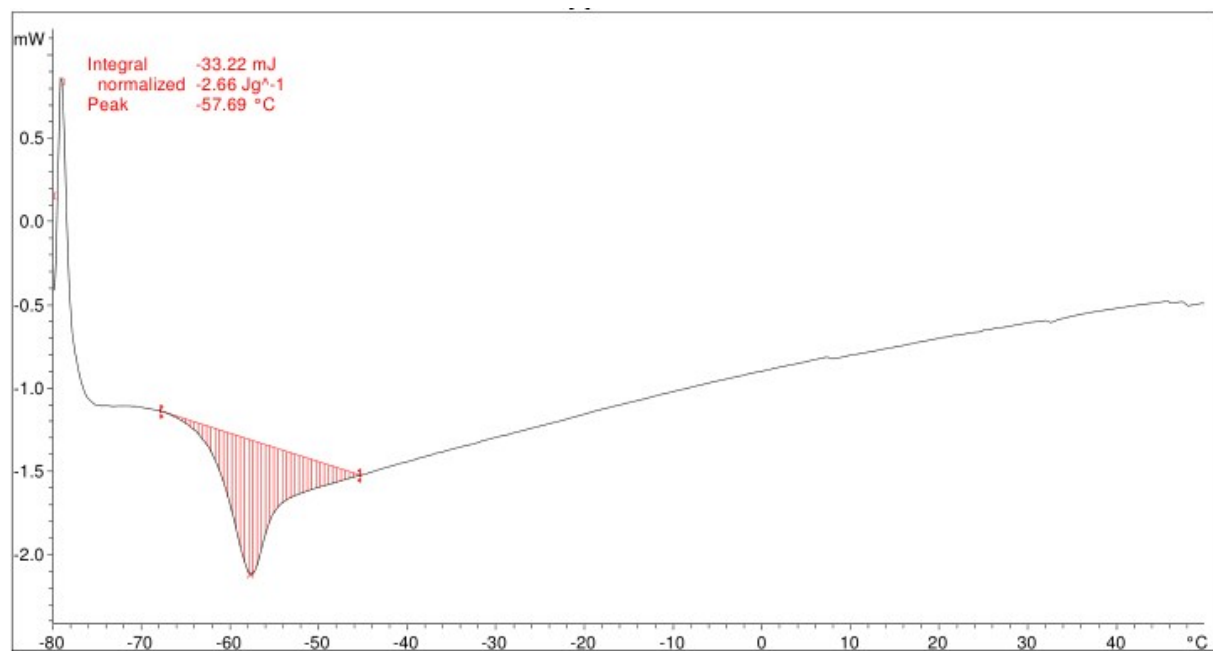


Fig B5 DSC spectra of **IL5**.

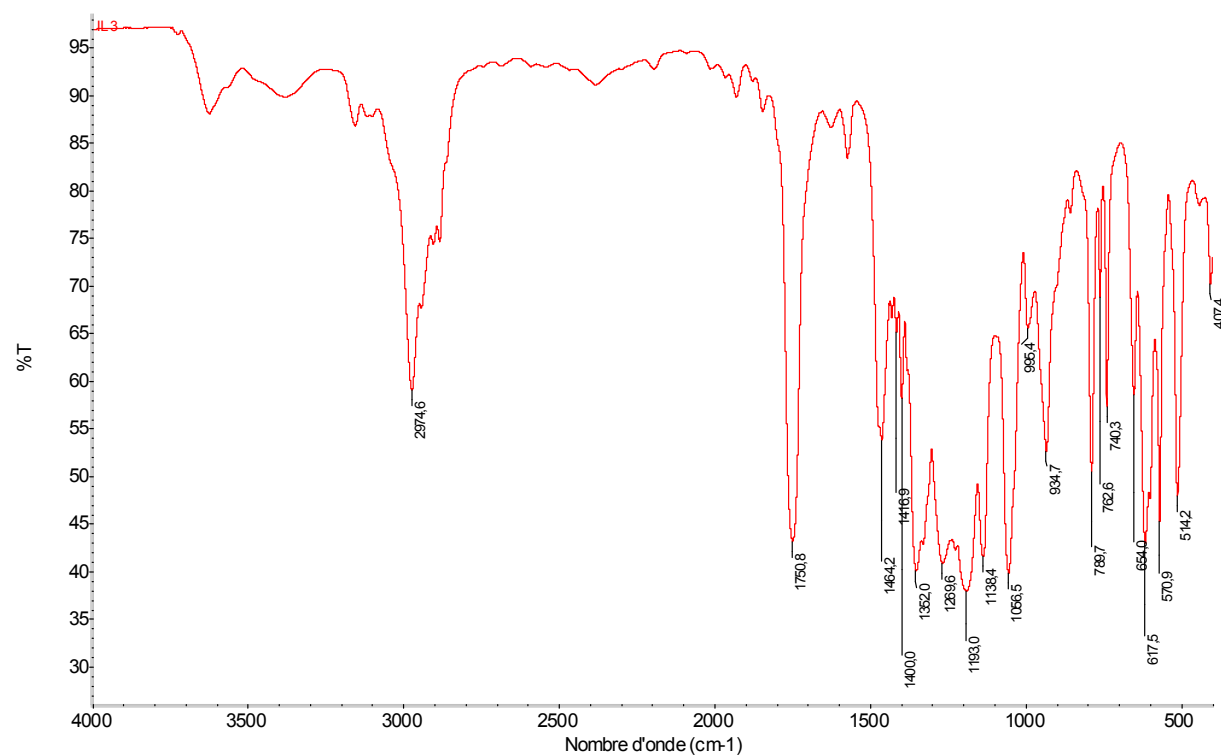
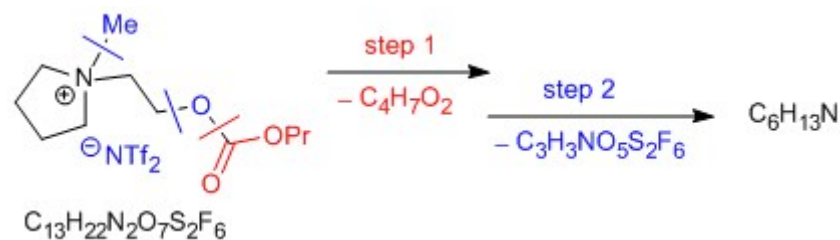
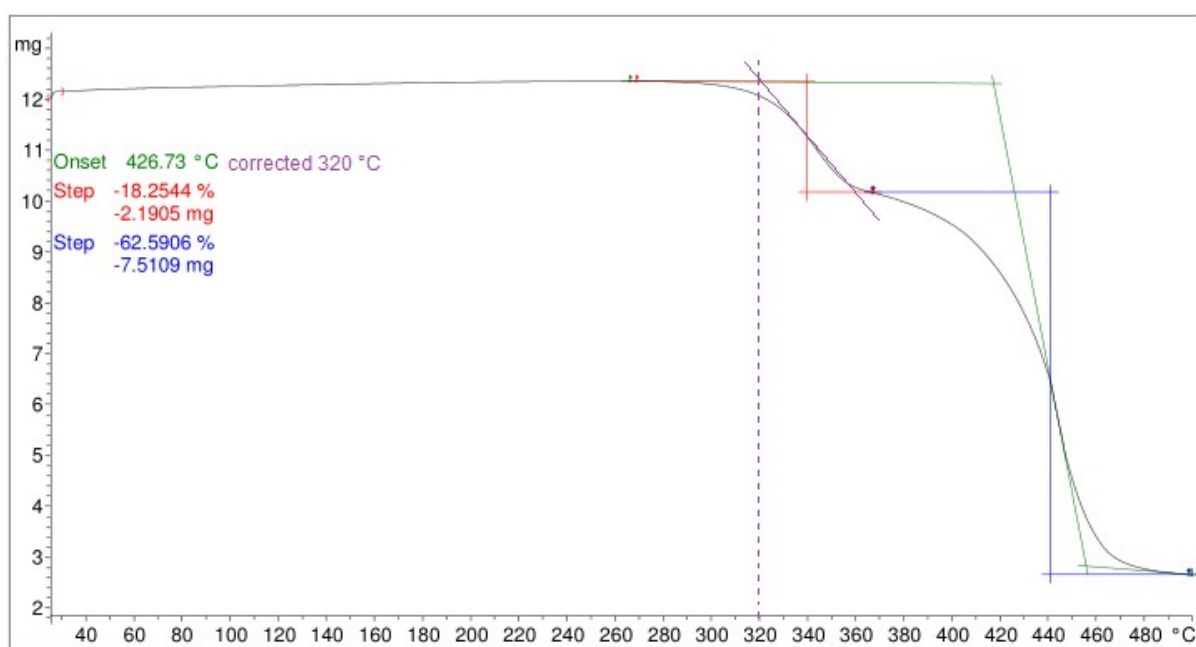


Fig B6 Infrared spectra of **IL5**.



| C ₁₃ H ₂₂ N ₂ O ₇ S ₂ F ₆ (5) | m _{lost} theor. | m _{lost} found |
|---|--------------------------|-------------------------|
| Step 1: C ₄ H ₇ O ₂ | 17.5 % | 18.3 % |
| Step 2: C ₃ H ₃ NO ₅ S ₂ F ₆ | 62.7 % | 62.6 % |
| Σm _{lost} | 80.2 % | 80.9 % |

Fig B7 Thermogram of **IL5** demonstrates onset point, corrected onset point and two steps of decomposition.

Appendix C

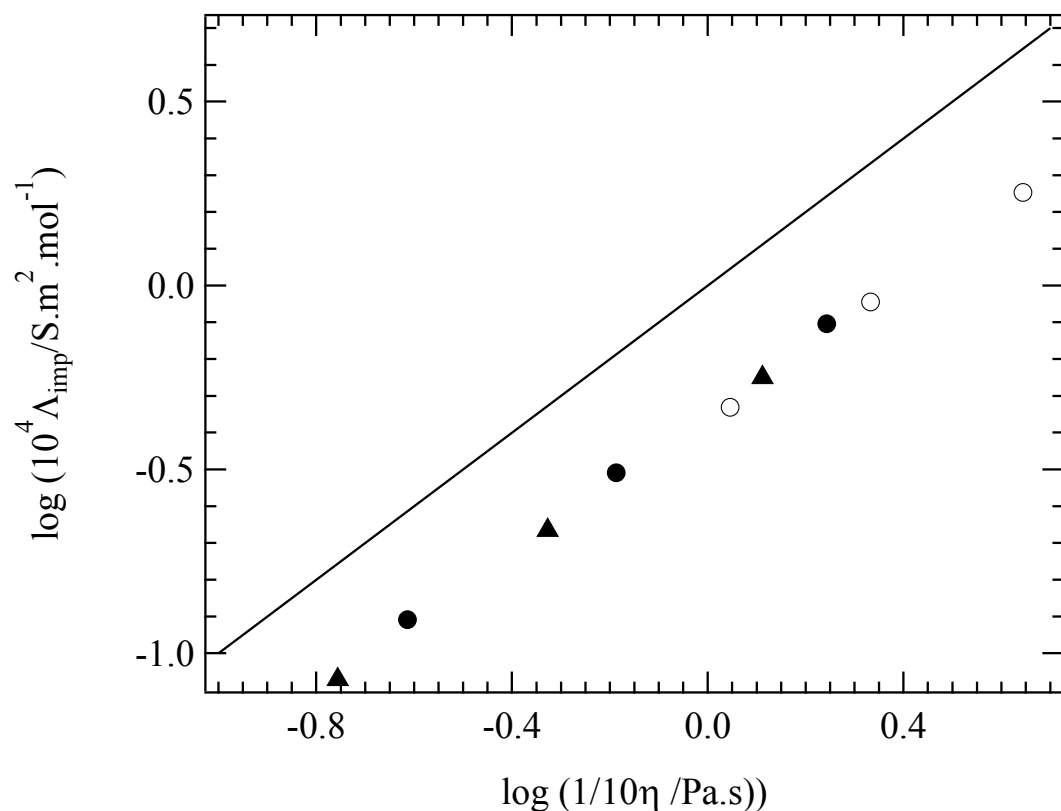


Fig C1 Walden plots of **IL4** (○), **IL5** (□) and $[\text{C}_8\text{C}_1\text{ImNTf}_2]^1$ (△) as a function of temperature from 298K to 333K. Black line, reference line (KCl, 0.01 M).

References

1. H. Tokuda, S. Tsuzuki, M. A. B. H. Susan, K. Hayamizu and M. Watanabe, *J. Phys. Chem. B*, 2006, **110**, 19593-19600.